



Minerals limit the deep soil respiration response to warming in a tropical Andisol

Casey R. McGrath · Caitlin E. Hicks Pries ·
Nhu Nguyen · Brian Glazer · Stanley Lio ·
Susan E. Crow

Received: 14 March 2022 / Accepted: 9 August 2022 / Published online: 7 September 2022
© The Author(s) 2022

Abstract Tropical regions hold one third of the world's soil organic carbon, but few experiments have warmed tropical soils *in situ*. The vulnerability of these soils to climate change-induced losses is uncertain with many hypothesizing these soils would be less sensitive to climate change because already-high temperatures in tropical systems might limit microbial sensitivity or due to increased mineral protection

Responsible Editor: Steven J. Hall.

Supplementary Information The online version contains supplementary material available at <https://doi.org/10.1007/s10533-022-00965-1>.

C. R. McGrath
Pacific Northwest National Laboratory, Richland,
WA 99354, USA
e-mail: casey.mcgrath@pnnl.gov

C. E. Hicks Pries
Department of Biological Sciences, Dartmouth College,
Hanover, NH 03755, USA

N. Nguyen
Department of Tropical Plant and Soil Sciences,
University of Hawaii Manoa, Honolulu, HI 96822, USA

B. Glazer · S. Lio
Department of Oceanography, University of Hawaii
Manoa, Honolulu, HI 96822, USA

S. E. Crow
Department of Natural Resources and Environmental
Management, University of Hawaii Manoa, Honolulu,
HI 96822, USA

of organic carbon in highly weathered tropical soils. Here we present the results of a deep soil (0–100 cm) warming experiment in a tropical Andisol. Andisols can store large, persistent pools of soil carbon that are protected from decomposition by poorly and non-crystalline minerals (PNCM). In 20 cm depth intervals, we measured key soil properties including carbon, nitrogen, pH, PNCM, bacterial and fungal richness along with temperature, moisture, and CO₂ production. Over a year of soil warming, CO₂ production significantly increased by 50–300% per degree of warming, but only in the top 40 cm of the soil profile in contrast to the results of other deep soil warming experiments. Multimodal analysis supported our hypothesis that high concentrations of PNCM was the primary driver of the lack of CO₂ response, followed by high relative soil moisture and low bacterial richness, which may be a proxy for organic carbon availability. The lack of elevated CO₂ production in response to warming suggests a limited positive feedback to climate change in Andisols driven by their strong mineral protection of organic matter. Therefore, Andisols should be considered high priority restoration or protection areas when considering the management of soil carbon stocks as part of climate action.

Keywords Warming · Soil carbon · Andisols · Tropical soils · Deep soils · Hawaii · Poorly crystalline and noncrystalline minerals

Introduction

The soil reservoir holds more carbon (C) than all terrestrial biomass and the atmosphere combined but is increasingly vulnerable to warming-induced losses in carbon stocks, which would be a positive feedback to climate change (Field and Raupach 2004; Davidson and Janssens 2006). The IPCC “business-as-usual-model” model (RCP 8.5) predicts global average air and soil temperatures will increase 4 °C by 2100. While more than 80% of the world’s soil organic carbon (SOC) exists below 20 cm (Jobbágy and Jackson 2000), depth will not protect it from warming—CMIP5 projections indicate the same amount of warming throughout the top meter of soil (Pachauri et al. 2015; Soong et al. 2020). In response, Torn et al. (2015) recently called for an international network of deep soil manipulation experiments (iSEN) to understand the response of soil carbon throughout the soil profile to climate change. One of the first experiments warming the whole soil profile indicated deep soils have the potential to become a large positive feedback to climate change as soil respiration throughout the soil profile increased by 30–34% and subsoil carbon storage decreased by 33% in response to 4 °C of warming (Hicks Pries et al. 2017; Soong et al. 2021). Evidence from temperate and boreal soils show increasing soil temperature escalates soil microbial activity and, consequently, soil respiration rates throughout the soil profile, causing declining soil C stocks where decomposition losses outweigh input gains (Hanson et al. 2017, 2020; Soong et al. 2021).

Tropical soils hold one third of the world’s SOC (Jobbágy and Jackson 2000), but few experiments warm tropical soils (Nottingham et al. 2019, 2020; Kimball et al. 2018). Historically, soil warming experiments focused on temperate and boreal systems (Plaza et al. 2019; Schädel et al. 2018). Lower latitude soils were hypothesized to be less vulnerable to rising temperatures due to the smaller absolute magnitude of warming they will experience and the increased mineral protection of organic matter in highly weathered tropical soils (Koven et al. 2017; Haaf et al. 2021). Initial predictions also hypothesized that tropical systems experiencing warm mean annual temperatures (MAT) under isothermic conditions would have little microbial response to warming as microbes might be approaching their biochemical thermal optima (Wood et al. 2012). However, model

projections indicate unprecedented increases in tropical surface temperatures (Diffenbaugh and Scherer 2011), and soil incubations have found no evidence of biochemical thermal optima occurring at these projected temperatures (Wood et al. 2012). Cavalieri et al. (2015) thus highlighted the urgent need for tropical deep soil warming experiments, given the high uncertainty of their SOC response to rising soil temperatures. Limited experimental evidence now shows that tropical soils do behave more like their temperate and boreal counterparts (Hicks Pries et al. 2017; Hanson et al. 2020), respiring significantly more CO₂ in response to soil warming (Zimmermann et al. 2010; Nottingham et al. 2020). The temperature sensitivity of soil respiration could lead to decreased soil carbon storage in tropical soils as observed along elevational gradients wherein carbon storage is greatest at higher, cooler elevations (Nottingham et al. 2015). In fact, one study suggests that tropical forests may be more sensitive to increases in temperature than higher latitudes, becoming large C sources (Mau et al. 2018).

Tropical soils store a larger proportion of their carbon in mineral-associations than temperate soils (Heckman et al. 2022). Recent meta-analyses (Heckman et al. 2022; Rocci et al. 2021) and experiments (Soong et al. 2021) suggest that mineral-associated carbon is less vulnerable to warming-induced losses than particulate carbon because sorption to soil minerals may offer some protection from microbial enzymatic attack. One critical end member soil lacking within soil warming experiments are volcanic-ash derived Andisols (WRB classification: Andosol), which are known for their strong mineral protection of soil organic matter (Torn et al. 1997). Andisols hold a disproportionate amount of soil carbon, storing 5% of the world’s soil carbon despite making up less than 1% of the world’s soils by area (Matus et al. 2014). Organo-mineral complexes are abundant in andic soils (Post and Kwon 2000; Torn et al. 1997). One recent study across a MAT gradient of Hawaiian Andisols suggested that Al and Fe poorly- and non-crystalline minerals (PNCM) have strong soil C-protection mechanisms leading to large soil C stocks (Giardina et al. 2014). However, whether the high degree of protection by PNCM will limit the response of soil C in Andisols to the intense warming predicted by 2100 is unknown.

Here we present one of the first deep soil warming experiments in a tropical soil and the first in an

Andisol. In contrast to most temperate and boreal systems, we hypothesized that the response of soil respiration to warming would saturate, indicating a threshold warming response controlled by poorly and non-crystalline minerals (PNCM), especially at depth. We tested this hypothesis in a wet montane tropical forest cleared of most vegetation using regression experimental design in which 50 locations across a hillslope were randomly subjected to warming along a gradient from ambient to +4 °C and soil respiration was quantified weekly within five depth intervals (0–20, 20–40, 40–60, 60–80, and 80–100 cm).

Materials and methods

Field site description

The field site was located at the Lyon Arboretum, Honolulu, HI (21.3330° N, 157.8015° W), which has a mean annual temperature of 25.6 °C within an isothermic soil temperature regime and 4200 mm of precipitation annually (Fig. S1). The arboretum is a forest ecosystem focusing on plants native to the Pacific Islands/Asian region, but over a century ago, the land was used for cattle grazing. We selected the field site for its soil type (Medial over pumiceous or cindery, ferrihydritic, isothermic Typic Hapludands) and access to electricity. In June 2017, we manually cleared the site of invasive *Hedychium flavescens* understory vegetation for ease of access. Some shallow-rooted grasses (*Eremochloa ophiuroides*, *Stenotaphrum secundatum*; max rooting depth of 15 cm) were kept to mitigate soil erosion, and the site was cleared of overstory trees. We realize that removing vegetation caused a disturbance. Thus, we waited a year before beginning the warming experiment (Fig. S3) and mapped soil respiration across the hillslope to avoid any potential decomposition hotspots created by the disturbance (Fig. S1). We maintained the site by cutting any *Hedychium flavescens* at the base until regrowth ceased and thinning the shallow-rooted grasses to prevent them from overtaking the field site.

Experimental design

We measured surface soil respiration rates across the hillslope for 1 year before initiating the warming treatment to inform the regression experimental design.

Sixty-four static chambers in a 2×2 m grid were sampled biweekly and interpolated into heatmaps using MATLAB to identify “hotspots” of microbial activity. Five blocks of equal surface area and initial surface respiration rates were placed across the hillslope to create a randomized block design. Areas of existing “hotspots” were not included in the blocking scheme to ensure a relatively homogenous initial surface soil respiration flux before starting the heating treatment (Fig. S1). Each block contained a single 2.5 m deep heating rod designed to create a gradient of heating across each block. Two sampling locations for each sampling depth interval (0–20, 20–40, 40–60, 60–80, and 80–100 cm) were randomly assigned to each block for measuring soil temperature, soil moisture, and soil respiration. Because this gradient design did not evenly heat across space, each sampling point experienced diffusion of CO₂ from its warmer side that was likely balanced by diffusion of CO₂ towards its cooler side. At each gas well set, soil temperature was recorded by the novel soil temperature sensors at the depth of interest (bottom of depth interval). The temperature sensors consisted of a single high accuracy digital sensor mounted on a board (TSYS01 TE Connectivity, Switzerland, custom made by UH Manoa MESH lab) and enclosed in a 3 ml polystyrene test tubes filled with epoxy that reported soil temperature every 30 s to an online server. Soil moisture was measured using a Sentek Diviner 2000 1.6 m rod (Sentek, Australia) at 30 static locations across the hillslope due to cost limitations. We assigned each gas well to its closest Diviner rod.

We installed five heating rods vertically into the soil to create a gradient of soil warming across the hillslope depending on distance from the rods. The rods were fabricated from 1.9 cm electric metallic tube conduit enclosing 2.5 m of heating cable (120 V, 10 W/ft, Brisk Heating SLCAB Self Regulating cable) and backfilled the conduit with sand to promote conductance. The heating rods were controlled by a PID controller that maintained the level of heating at +4 °C above ambient with a monitoring sensor 70 cm away from the rod placed 60 cm into the soil profile. Ambient temperature was calculated by averaging four temperature sensors outside the expected radius of heating (3 m away from rods and 60 cm deep). The temperature sensors consisted of a single high accuracy digital sensor mounted on a board (TSYS01, custom made by UH

Manoa MESH lab) and enclosed in a 3 ml polystyrene test tubes filled with epoxy that reported soil temperature every 30 s to an online server.

We were able to maintain the targeted range of 0 to +4 °C differences in mean soil temperatures between ambient and heated areas from November 2018 through November 2019 (Fig. S2). There were several inconsistencies in the soil warming across time because the heaters were turned off due to site vandalism in December 2018 and internet connectivity problems in February and July 2019. Even though the average ambient soil temperature varied throughout the year, soil temperature data shows we were able to maintain +4 °C at the target radius (70 cm) and depth of heating (60 cm) for > 90% of the time preserving the target gradient of soil temperatures.

Soil CO₂ production

Weekly sampling of soil CO₂ concentrations, soil temperature, and soil moisture took place November 2018 through November 2019. At each sampling location, gas wells (0.635 cm stainless steel seamless tubing) were installed at a 45° angle in sets of three: at the depth of interest, the depth of interest – 20 cm, and the depth of interest + 20 cm. We sampled 5 ml of gas from each gas well into evacuated vials, whose CO₂ concentrations were then analyzed on a Shimadzu GC-2014 (Shimadzu USA Manufacturing Inc, Canby, OR). A surface static chamber (10 cm diameter × 30 cm high PVC collar covered with a PVC cap installed with a septum during gas sampling) was used to measure the flux density across 0 cm (i.e., the surface respiration flux) needed to calculate CO₂ production within the 0–20 cm depth interval (see below).

Using the CO₂ concentrations at each depth, we calculated CO₂ production within each depth using the following series of equations based on Fick's Law (Tang et al. 2003; Moyes and Bowling 2013; Contosta et al. 2016; Hicks Pries et al. 2017) (Eq. 1).

$$F = -D \frac{dC}{dz} \quad (1)$$

where F is the flux density (g m⁻³ h⁻¹), D is the diffusion coefficient, and dC/dz is the change in

concentration over depth. The diffusion coefficient was determined by Eq. 2:

$$D = D_{ao} \left(\frac{T}{293.15} \right)^{1.75} \left(\frac{101.3}{P} \right) \xi \quad (2)$$

where D is the diffusion coefficient of CO₂ in soil, T is the temperature in °C at the time of sampling, P is local atmospheric pressure in kPa, and ξ is a dimensionless tortuosity factor. The tortuosity equation was an empirical relationship chosen from Moyes and Bowling (2013) (Eq. 3).

$$\xi = 0.95 \varepsilon^{1.93} \quad (3)$$

where ε is the air-filled porosity derived from the total soil porosity, bulk density each depth, and volumetric water content at each sampling depth during the time of measurement. To calculate CO₂ production across a given depth interval, the flux densities across that interval were calculated by subtracting the flux density of the lower depth from the flux density of the upper depth and then dividing by the 20 cm depth increment. CO₂ production is the soil respiration occurring within that depth interval, which is a mixture of root, root-derived, and microbial respiration.

Soil characterization

Initial soil cores (0.8 in diameter, 100 cm depth) were taken in May 2018, after site clearing and 6 months before soil warming at each of the 50 sampling locations to characterize the carbon (C), nitrogen (N), poorly- and non-crystalline minerals (PNCM), organo-mineral complexes, active Fe ratio, pH, ΔpH, and the richness of the microbial communities based on 16S and ITS sequences. 16S rRNA analysis provided genus-level information on bacteria while ITS analysis resulted in fungal inventory (see below for information on DNA extraction). We present only the data from samples that corresponded with the depth interval measured at each sampling location. Accurately sampling 50 1-m deep soil profiles for bulk density was not logistically possible and would create disturbances. Therefore we estimated bulk density at each of the 50 sampling locations by dividing the dry weight of the core sample (g) by the volume of the core (cm³). Soil cores were split into 0–20, 20–40, 40–60, 60–80, and 80–100 cm depths for the analyses. C and N were analyzed on dried, ground soil with

a Carlo Erba NC 2500 Elemental Combustion System (Thermo Fisher Scientific, Waltham, MA). Three different extraction methods were used to determine the Fe and Al content: hydroxylamine hydrochloride (Ross et al. 1985), citrate dithionite (Holmgren 1967), sodium pyrophosphate (McKeague 1967). Hydroxylamine hydrochloride extraction was chosen in place of ammonium oxalate because it dissolves sustainably lower amounts of crystalline oxides (like magnetite common in Hawaii's volcanic soils) (Silva et al 2015; Chao and Zhou 1983; Ross et al. 1985). The extracted analytes were then measured using Inductively Coupled Plasma analysis (ICP). PNCM was calculated as the hydroxylamine hydrochloride extractable Al+0.5Fe molar quantities per gram soil. Fe and Al organo-mineral complexes were calculated from the sodium pyrophosphate extraction. The active Fe ratio was calculated from the hydroxylamine hydrochloride extractable Fe divided by the citrate dithionite extractable Fe. pH was determined by using a 2:1 MilliQ water to soil ratio and measured using a Thermo Scientific benchtop pH meter. ΔpH was determined by the deionized water method—KCl method (1 M KCl, 2:1 KCl to soil ratio). ΔpH is a proxy of the organo-mineral association potential with a negative ΔpH indicating adsorption is more likely. The relative charges of the mineral and OM particles are dependent on soil pH via the point of net zero charge (pzc). Soils with OM above the pzc but minerals below the pzc will have oppositely charged particles resulting in adsorption. Soil minerals above the pzc (indicated by ΔpH greater than 0 in more acidic soils) will have positively charged OM and mineral particles, making adsorption less likely (Bailey et al. 2019).

DNA was extracted from 0.25 g of each soil sample using the Qiagen DNeasy PowerSoil Kit. Bacterial 16S (V4 region) rRNA genes were sequenced using the primer pairs 515F (Parada et al. 2016) and 806R (Apprill et al. 2015) using a dual-barcoding approach. For fungi, the ITS1 region was targeted using primer pairs ITS1F (White et al. 1990) and ITS2 (Gardes and Bruns 1993) using a single barcode on the ITS2 primer (Smith and Peay 2014). Amplified samples were pooled in equimolar concentrations and sequenced together as a single run using the Illumina MiSeq PE250 at the University of California, Berkeley QB3 Genomics center. Bioinformatics processing of the sequences was performed using QIIME2 (Bolyen et al. 2019) and an established pipeline

(Nguyen et al. 2016) that uses stringent filtering criteria to minimize noise. For bacterial sequences, DADA2 exact sequence variance were considered as OTUs (operational taxonomic units) and fungal exact sequence variance were further clustered at 97% to obtain the best fungal OTUs.

Data analysis

First, we performed one-way ANOVAs with depth as a categorical main effect in R (R Core Team 2021). A significant depth effect was followed by a tukey post hoc test to determine which depths differed from one another. We used a Bonferroni correction of our alpha to account for the number of tests performed (13), so a significant effect had a $p < 0.0036$. Our response variables included the initial soil characterization data and the mean values of soil moisture (VWC), soil temperature, and soil CO₂ production at the 50 sampling locations averaged over time. For the soil temperature data, Δ soil temperature (mean soil temperature – mean ambient soil temperature) at each sampling location was used as a measure of the soil warming treatment. Soil CO₂ production was log transformed to meet assumptions of the ANOVA. Next, we completed a principal component analysis (PCA) using the same response variables to inform the parameters chosen for a multiple regression (prcomp function, R Core Team 2021). The PCA highlighted potential drivers of spatial variability and the importance of depth, supporting the need for regressions that included soil depth.

In order to model the most significant factors affecting the response of CO₂ production across depths, we used generalized additive modeling (GAM) since it is robust to both parametric and non-parametric data (Hastie and Tibshirani 1986). Furthermore, our hypothesis predicted a non-linear response of CO₂ production to temperature, which a GAM can capture. The GAM structure can be written as Eqs. 4:

$$g(E(Y)) = \alpha + s_1(x_1) + \dots + s_p(x_p) \quad (4)$$

where Y is the response variable, E(Y) is the predicted value, and $s_1(x_1) + \dots + s_p(x_p)$ are the estimated non-parametric variables fit with a smoothing function.

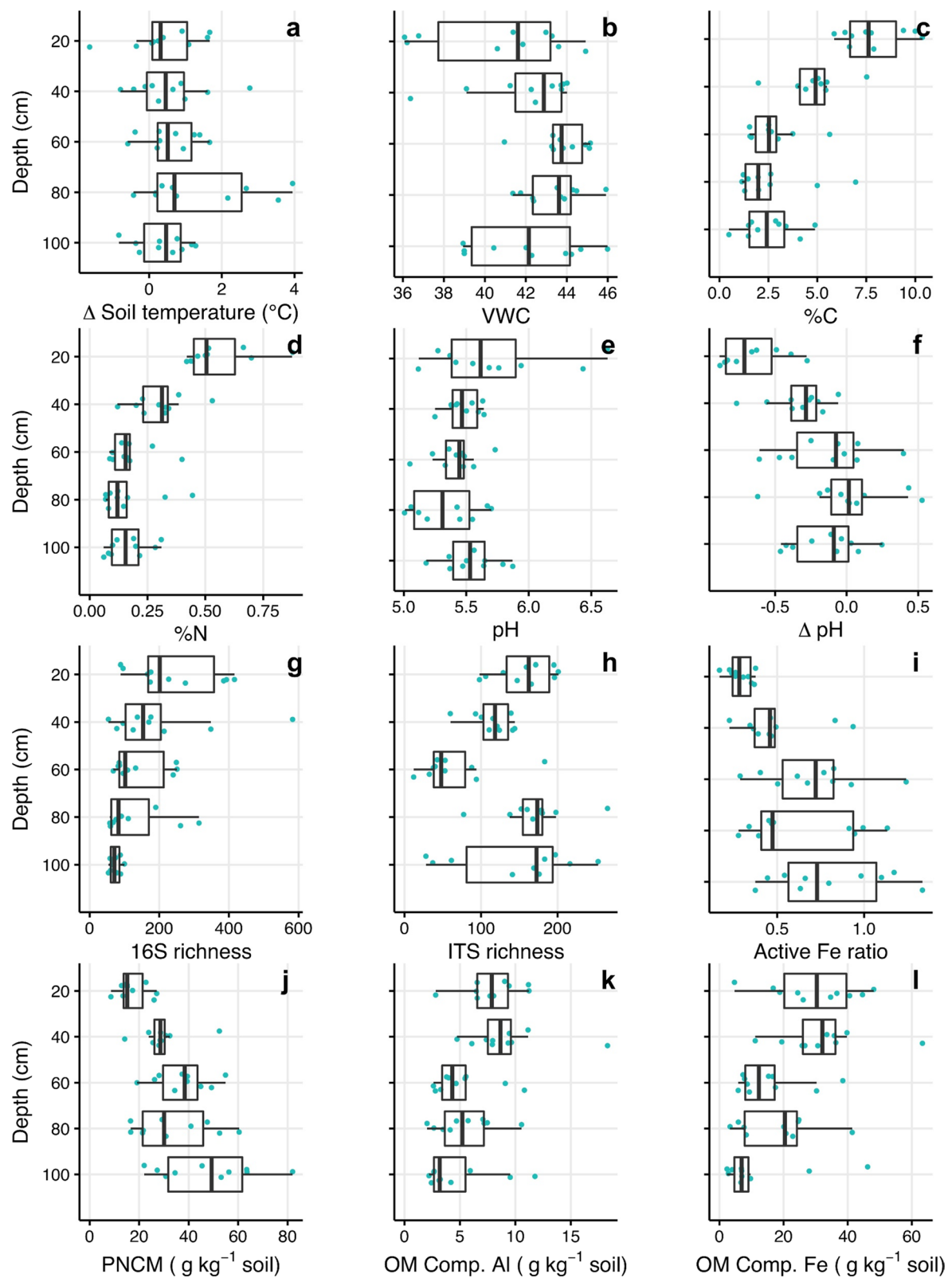


Fig. 1 Depth wise changes in warming treatment (Δ soil temperature), volumetric water content (VWC), carbon (C), nitrogen (N), pH, Δ pH, 16S and ITS-based microbial community richness, active Fe ratio, poorly crystalline and non-crystalline minerals (PNCM), and organically complexed (OM Comp.) Al (k) and Fe (l). The warming treatment and VWC were averaged over November 2018 through November 2019 for each depth interval. The middle lines are the medians, the boxes are the 25th to 75th percentiles, and the whiskers are 1.5 times the interquartile range

First, a global model combining the data from all depths was developed utilizing the “mgcv” package in R (Wood 2006) with the temporal means of CO_2 production, VWC, and soil warming as well as C, N, pH, Δ pH, PNCM, active Fe ratio, OM complexed Al, OM complexed Fe, 16S richness, and ITS richness across all 50 sampling locations, each of which is a specific depth interval. To optimize the fit of the model, we log transformed the response variable, CO_2 production. We checked the concavity of predictors in this global model and dropped one from each pair of variables that had a concavity value > 0.8 . We then reran the global model without N (related to C), active Fe ratio (related to PNCM), and OM-complexed Al (related to OM-complexed Fe).

Next, we wanted to test how the controls on CO_2 production differ with depth. The global model was limited by the number of smoothers (k) and therefore was unable to accommodate modeling by each of the sampling depths. When optimizing models for each depth, the number of smoothers limited the number of terms included in the model to four. Fitting by AIC determined that three smoothers (k) per model term limited underfitting while including the maximum terms for the optimal model. Given these limitations, four terms could be included in the depth-wise model. We set the soil warming treatment, Δ soil temperature, as one of these terms and then iterated the model through all possible model combinations with three other terms (chosen from among VWC, C, pH, Δ pH, PNCM, Fe-organic complexes, 16S richness, and ITS richness), each with three smoothers, by five depth groupings (0–20, 20–40, 40–60, 60–80, and 80–100 cm) for a total of 56 model combinations. Model selection was completed by Akaike information criterion (AIC) utilizing the “MuMin” package in R (Barton 2019; Peters et al. 2019). Within this manual model iteration by depth grouping, the top model was selected based on the corrected Akaike

information criterion (AICc) threshold below used for small sample sizes ($n < 100$) (Takezawa 2014):

$$\Delta i = \text{AICc}_i - \text{AICc}_{\min} \quad (5)$$

where AICc_i is the AICc for the i th model, and AICc_{\min} is the minimum of AICc for all model candidates. The optimal model is $\Delta i = \Delta_{\min} = 0$ (Burnham and Anderson 2003). Therefore, the model with the lowest AICc was selected as the “best model” for representing the system.

Results

Many of the soil characteristics significantly differed by depth including %C ($p < 0.0001$), %N ($p < 0.0001$), Δ pH ($p < 0.0001$), ITS richness ($p = 0.00017$), active Fe ratio ($p = 0.0006$), PNCM ($p = 0.0001$), and OM-complexed Fe ($p = 0.003$); however, the temperature treatment (Δ Temp; $p = 0.20$), VWC ($p = 0.046$), pH ($p = 0.043$), OM-complexed Al ($p = 0.006$), and the 16S richness ($p = 0.0097$) did not based on the bonferroni-adjusted alpha of 0.0036($df = 4$, $n = 50$ for all; Fig. 1). Soil respiration decreased significantly with depth; the most significant differences were between the surface 0–20 cm and bottom 60–100 cm depths ($p < 0.0001$, $df = 4$, $n = 50$; Fig. 2a). The amount of PNCM per gram of soil C increased significantly with depth ($p = 0.003$, $df = 4$, $n = 50$; Fig. 2b). The PCA of the temporally averaged (November 2018 to November 2019) and initial soil parameters explained 59% of the variance in the data within the first two principal components (Fig. 3; Table S1). The first principal component, which explained 42% of the variance, shows a gradient across depth with the shallowest sampling depth, 20 cm, having a strong correlation with CO_2 production and soil C and N. Sampling depths below 40 cm were strongly correlated with the concentration of PNCM, the active Fe ratio, and Δ pH, the proxy index for net mineral charge.

The global model of the controls on CO_2 production explained 91.7% of the model deviance ($R^2 = 0.87$). The most significant term from the global model was depth ($p < 0.0001$; Table 1). Other significant terms included soil warming (Δ Temp; $p = 0.0033$), VWC ($p = 0.024$), Δ pH ($p = 0.027$), and %C, which was nearly significant ($p = 0.066$; Table 1). As expected, CO_2 production increased

Fig. 2 The natural log of CO_2 production averaged over November 2018 through November 2019 for each depth interval (a) and the amount of poorly and non crystalline minerals per g soil carbon within each depth interval (b). The middle lines are the medians, the boxes are the 25th to 75th percentiles, and the whiskers are 1.5 times the interquartile range. One way ANOVA, depth effect, $Df=4$, $n=50$, $p<0.0001$ for a and $p=0.003$ for b)

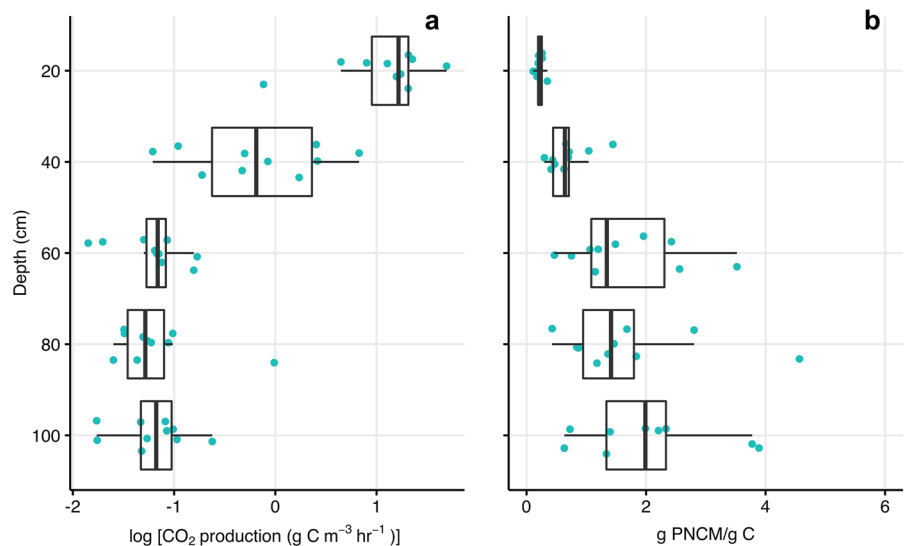
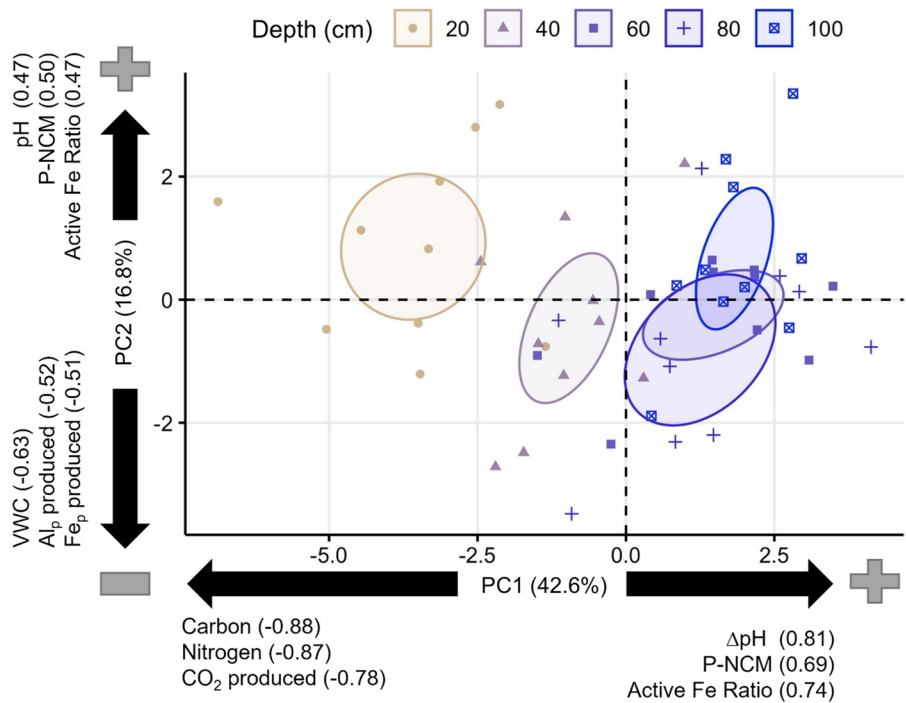


Fig. 3 First and second principal components from the mean timeseries and initial soil characterization datasets for the Lyon Arboretum field site. Top three positive and negative variables from the correlation matrix are listed for each principal component with corresponding correlation values



with the amount of soil warming and carbon content of the soil (Fig. 4a, c). In contrast, CO_2 production decreased with increasing volumetric water content and depth (Fig. 4b, e). ΔpH increased the amount of CO_2 produced until ΔpH around 0 after which it had little effect (Fig. 4d).

Given the high significance of depth in the global model and in the PCA visualization, further model

optimization by depth was needed. Model optimization provided three key predictors when included with the soil warming treatment and factored by five depth groupings (0–20, 20–40, 40–60, 60–80, and 80–100 cm). These key predictors were VWC, PNCM concentration, and the bacterial OTU (16S) richness ($R^2=0.93$, Deviance explained = 96.8%, $n=50$; Fig. 4, Table 1). Soil CO_2 production

Table 1 Approximate significance of the smoothed terms from the best fit model by depth grouping (0–20, 20–40, 40–60, 60–80 and 80–100 cm), which had the following formula: $\log(\text{CO}_2) \sim s(\Delta \text{ soil temperature}, k=3, \text{by}=\text{depth}) + s(\text{vwc}, k=3, \text{by}=\text{depth}) + s(\text{P-NCM}, k=3, \text{by}=\text{depth}) + s(\text{S_16S}, k=3, \text{by}=\text{depth})$

Smoothed terms	edf	Ref.df	F	p-value
s(Δ soil temp): depth 0–20	1.00	1.00	13.2	0.0015
s(Δ soil temp): depth 20–40	1.00	1.00	45.1	<0.0001
s(Δ soil temp): depth 40–60	1.00	1.00	2.67	0.12
s(Δ soil temp): depth 60–80	1.45	1.69	1.64	0.18
s(Δ soil temp): depth 80–100	1.00	1.00	0.17	0.69
s(vwc): depth 0–20	1.00	1.00	0.500	0.48
s(vwc): depth 20–40	1.00	1.00	44.8	<0.0001
s(vwc): depth 40–60	1.84	1.97	5.37	0.013
s(vwc): depth 60–80	1.00	1.00	15.8	0.00064
s(vwc): depth 80–100	1.79	1.96	2.27	0.16
s(P-NCM): depth 0–20	1.95	2.00	61.6	<0.0001
s(P-NCM): depth 20–40	1.95	1.99	13.1	0.0021
s(P-NCM): depth 40–60	1.00	1.00	1.17	0.29
s(P-NCM): depth 60–80	1.92	1.99	6.75	0.0049
s(P-NCM): depth 80–100	1.00	1.00	0.08	0.78
s(S_16S): depth 0–20	1.00	1.00	10.94	0.0032
s(S_16S): depth 20–40	1.93	1.99	8.51	0.0024
s(S_16S): depth 40–60	1.00	1.00	2.81	0.11
s(S_16S): depth 60–80	1.67	1.88	5.30	0.010
s(S_16S): depth 80–100	1.00	1.00	6.06	0.022

Overall model statistics were: $R^2=0.93$, Deviance explained=96.8%, n=50). Significant p-values <0.05 are bolded

increased significantly with the warming treatment in the surface 0–20 and 20–40 cm depths, but not in the deeper soil (Fig. 5a). As in the global model, CO_2 production decreased with increasing VWC; an effect that was significant in the 20–40, 40–60, and 60–80 cm depths (Fig. 5b). CO_2 production significantly declined with PNCM content in the surface soil only and had idiosyncratic relationships in the deeper soil (Fig. 5c). For example, CO_2 production increased until about 40 g PNCM kg^{-1} after which it decreased at 20–40 and 60–80 cm depths, but had no significant relationships with PNCM content at 40–60 and 80–100 cm depths. Lastly, CO_2 production significantly increased with increasing bacterial OTU richness at 0–20, 60–80, and 80–100 cm depths (Fig. 5d).

Discussion

The importance of soil minerals in determining the soil warming response

Warming the whole profile of a tropical Andisol increased CO_2 production within the top 40 cm by 50–300% per 1 °C increase in temperature, but had no significant effect on CO_2 produced below 40 cm. Mineral protection, attributed to high concentrations of poorly and non-crystalline Al and Fe at depth, was likely the main factor inhibiting the temperature-dependent response of soil CO_2 production. The lack of a warming response at depth contrasts the results of the only other whole-soil-profile warming experiment to partition soil respiration by depth where a 4 °C increase in soil temperature led to a 37% increase in surface CO_2 flux with 40% of that response coming from deeper soils (Hicks Pries et al. 2017; Soong et al. 2021). In another whole-soil-profile tropical soil warming experiment, SWELTR, depth-resolved fluxes were not quantified; however, 4 °C of warming caused a substantial 55% increase in surface CO_2 flux (Nottingham et al. 2020). Our surface soils had an even larger response, with CO_2 production doubling in response to 2 °C of warming at 0–20 cm and increasing by a factor of 6 in response to 2 °C of warming at 20–40 cm. This strong response may have been driven in part by decaying root biomass as a result of our site preparation. Despite their much warmer climate, tropical soils can be just as responsive to warming as their temperate and arctic counterparts, at least in the short term (Lu et al. 2013; Wood et al. 2019).

The unresponsiveness of deep soil respiration to experimental warming demonstrates the importance of mineral-associations in reducing the susceptibility of SOM to climate change-driven losses (Rocci et al. 2021). Shallow SOM is often more accessible to soil microbes who can degrade it readily; whereas in deep soils, a greater proportion of the carbon is associated with soil minerals that can stabilize and protect SOM from microbial decomposition (Adhikari et al. 2019; Porras et al. 2018; Jackson et al. 2017). Hawaiian Andisols are known for their strong organo-mineral associations driven by high concentrations of poorly and non-crystalline minerals that protect carbon through sorption, aggregation, or co-precipitation reactions (Cismasu et al. 2015; Lalonde

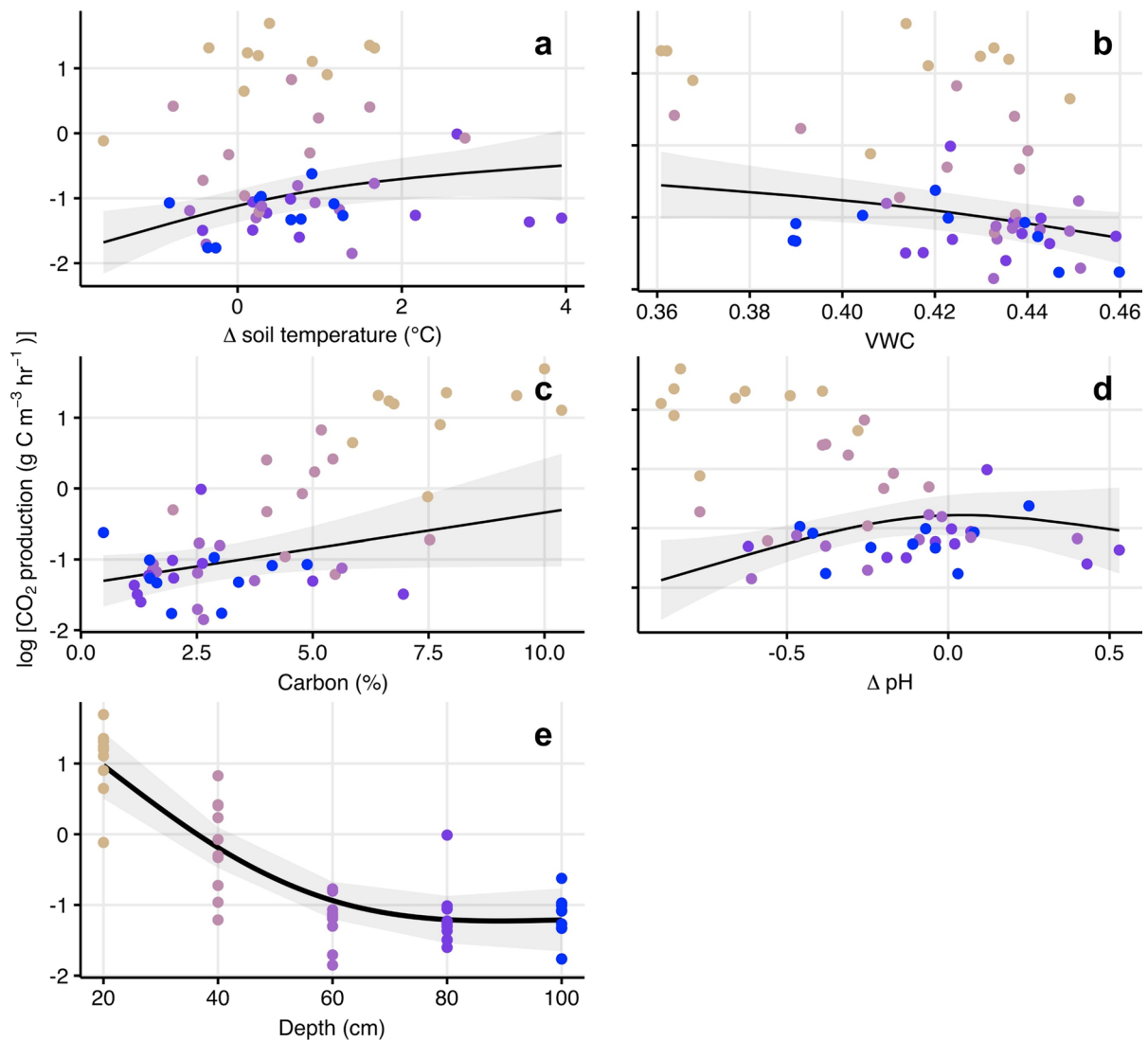


Fig. 4 Global GAM predictions for all significant predictors of log-transformed CO₂ production ($n=50$). Δ soil temperature (a), volumetric water content (VWC; b), Δ pH (d), and depth (e) are all significant predictors ($p<0.05$) and carbon (c) was marginally significant ($p<0.07$). The points are the data

colored by depth (see e for values), the lines are the predictions of each significant predictor with the other model variables held at their mean, and the grey ribbons are the 95% confidence intervals

et al. 2012) leading to long soil carbon residence times (Torn et al. 1997). These PNCM increased with depth in our soils and were a significant control on soil respiration at several depths such as at the surface where soil respiration declined with increasing PNCM. While we do not have direct measures of the amount of mineral-associated carbon in these soils, the average amount of PNCM per carbon increased by an order of magnitude from 0.2 g PNCM per g C

at 0–20 cm to 3 g of PNCM per g C at 80–100 cm, so carbon at depth had a greater likelihood of being mineral-associated (Fig. 2b). Soils with high concentrations of PNCM such as allophane, imogolite, and primary Al-OM complexes are common in Andisols and other soils derived from volcanic ash (Nanzyo 2002). Even at low concentrations, PNCM can protect OM from destabilization and decomposition (Kramer and Chadwick 2016). High concentrations of both PNCM

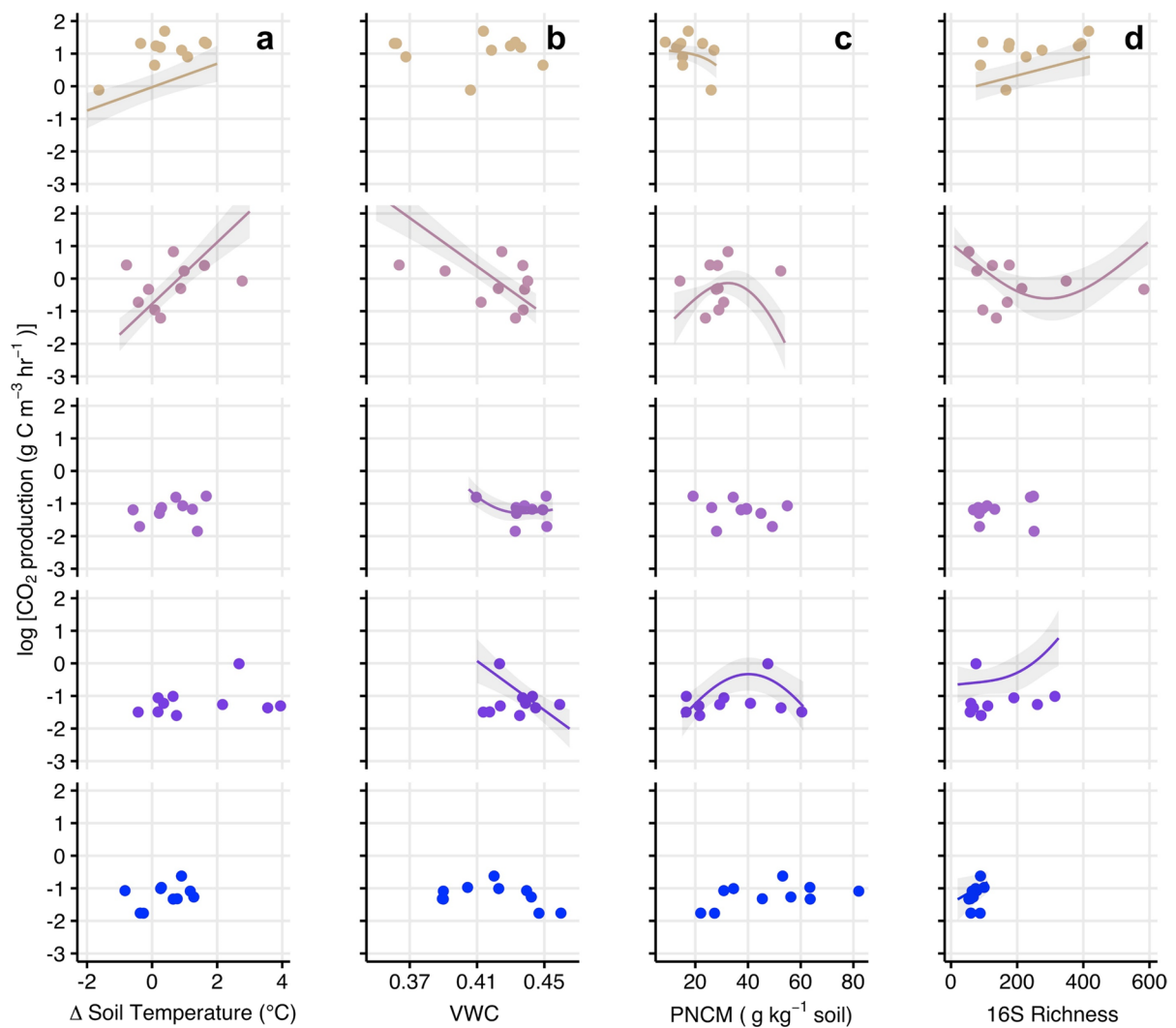


Fig. 5 Plot of each smoothed term for the top GAM model by depth (top to bottom: 0–20, 20–40, 40–60, 60–80, 80–100 cm) as predictors of log transformed CO_2 production. Δ soil temperature (**a**), VWC (volumetric water content; **b**), poorly crystalline and non-crystalline minerals (PNCM; **c**), and 16S-based

richness (**d**) were significant predictors in the depth wise GAM ($p < 0.05$). The points are the data colored by depth, the lines are the model predictions with the other model variables held at their mean for the given depth interval, and the grey ribbons are the 95% confidence intervals of the model predictions

and soil C typically persist over time deep in the soil profile of Hawaiian Andisols (e.g., Giardina et al. 2014). While the importance of PNCM in controlling carbon abundance and stabilization is well known (Giardina et al. 2014; Torn et al. 1997), this is the first study to demonstrate its importance in protecting soil carbon from loss when faced with climate warming.

The significant relationship of soil respiration to ΔpH in the global GAM model further supports the importance of organo-mineral associations in

controlling the response of soil respiration to warming. Soil respiration decreased with more negative ΔpH values below zero. ΔpH values less than zero indicates stronger mineral associations because minerals are more likely to have a net negative charge to facilitate adsorption of positively charged organic matter. At ΔpH greater than zero, where minerals and organic matter are less likely to have opposing charges weakening mineral protection of organic matter, there was an increase in soil respiration rates.

Organomineral associations also explain why our results contrast those of a previous whole soil warming experiment in a temperate forest. At that site, there was a very strong response of deeper soil respiration to warming driven by the large proportion of free particulate carbon at depth, which was preferentially lost relative to mineral-associated carbon over 5 years (Soong et al. 2021). That soil was developed from a granitic parent material, which had weaker mineral protection of organic carbon than nearby andesitic soils (Rasmussen et al. 2005) and had similar proportions of particulate and mineral-associated carbon throughout the soil profile (Hicks Pries et al. 2017).

Other drivers of CO₂ production throughout the profile

Soil moisture reduced CO₂ production. At this tropical site there are 4200 mm of precipitation a year leading to volumetric water contents of 20.8–49.4% throughout the year and greater than 35% annually. Other tropical soil respiration studies found soil moisture had a significant parabolic effect on CO₂ produced (Hashimoto et al. 2004; Wood et al. 2013). Interestingly, the tipping point of that relationship from positive to negative was a volumetric water content of 35% in Wood et al. (2013), the lowest average annual water content measured in this study. High volumetric water content indicates increased water-filled pore space that limits oxygen diffusion leading to anaerobic sites within the soil profile that can reduce microbial respiration (Silver et al. 1999; Henry 2012). Reduced diffusion of CO₂ out of the soil due to increased water-filled pore space, a mechanism sometimes cited for reductions in surface CO₂ production at high moisture levels (e.g., Wood and Silver 2012; Wood et al. 2013), was likely less of a factor in this study wherein CO₂ production was measured within individual depth increments via gas wells. In these very wet soils, soil moisture was not affected by soil warming as in other experiments (linear regression, df=48, p=0.51, n=50; Xu et al. 2013).

As expected, soil respiration increased with increasing soil carbon content. Unfortunately, we were unable to quantify the amount of carbon within the volume of each depth interval since a proxy was used to estimate bulk density due to logistical reasons. Bacterial richness, which was positively related

to soil carbon content (linear regression, p=0.016, n=50), was a significant predictor in the depth-wise model and, as with soil carbon concentrations, increased CO₂ production. It is unknown whether this effect was driven by bacterial diversity itself (Delgado-Baquerizo et al. 2016; Liu et al. 2018) or another metric that scales with bacterial diversity such as microbial biomass or carbon amount (Bastida et al. 2021). However, it should be noted that the relationship between microbial diversity and biomass is negative in tropical forests (Bastida et al. 2021). Overall, bacterial richness being significant in the depth-wise model instead of soil carbon indicates that bacterial richness may be a better indicator of carbon availability at our site than carbon itself. As previously stated, soil carbon at depth is more likely to be protected from microbial decomposition by minerals, decoupling the relationship between soil carbon and respiration in this tropical Andisol. The mechanisms by which microbial communities interact with mineralogical controls and soil carbon will be tested in future research at this site.

Conclusion

Understanding the feedbacks of soil respiration to rising global air temperatures provides critical information to climate models on how climate changes may impact the terrestrial carbon cycle. Climate change experiments in underrepresented soil and climate regimes must be expanded upon in order to develop an accurate projection of future of soil organic carbon storage and sequestration. This study piloted a low-cost methodology for warming and monitoring soils while adding to the lack of empirical evidence on the effects of soil warming in tropical soils and Andisols. Andisols are critical soils to be integrated into models given the demonstrated role of their unique mineralogy on SOC stabilization, which can be used to refine the relationship between mineral-protected carbon and temperature sensitivity.

Unlike any other deep soil warming experiment to date, there was no significant CO₂ response to soil warming below 40 cm of the profile. Multimodal analyses confirmed the hypothesis that high concentrations of PNCM was the primary driver in the lack of CO₂ response, followed by high relative soil moisture and low bacterial richness at depth. The lack of CO₂ response due to potential PNCM protection

suggests a limited positive feedback to warming within Andisols, especially at depth. Therefore, Andisols could be explored as a priority for restoration or protection areas when considering management and policy decisions for climate action.

Acknowledgements Support for this project comes from the Lyon Arboretum and the C-MĀIKI - Center for Microbiome Analysis through Island Knowledge and Investigation.

Funding This research was funded by USDA NIFA.

Data availability The datasets generated during and analyzed during the current study are available in the McGrath_ et_al_2022_Biogeochemistry GitHub repository, https://github.com/mcgrathc/McGrath_et_al_2022_Biogeochemistry.

Declarations

Conflict of interest The authors have not disclosed any competing interests.

Open Access This article is licensed under a Creative Commons Attribution 4.0 International License, which permits use, sharing, adaptation, distribution and reproduction in any medium or format, as long as you give appropriate credit to the original author(s) and the source, provide a link to the Creative Commons licence, and indicate if changes were made. The images or other third party material in this article are included in the article's Creative Commons licence, unless indicated otherwise in a credit line to the material. If material is not included in the article's Creative Commons licence and your intended use is not permitted by statutory regulation or exceeds the permitted use, you will need to obtain permission directly from the copyright holder. To view a copy of this licence, visit <http://creativecommons.org/licenses/by/4.0/>.

References

- Adhikari D, Dunham-Cheatham SM, Wordofa DN, Verburg P, Poulsen SR, Yang Y (2019) Aerobic respiration of mineral-bound organic carbon in a soil. *Sci Total Environ* 651:1253–1260. <https://doi.org/10.1016/j.scitotenv.2018.09.271>
- Apprill A, McNally S, Parsons R, Weber L (2015) Minor revision to V4 region SSU rRNA 806R gene primer greatly increases detection of SAR11 bacterioplankton. *Aquat Microb Ecol* 75(2):129–137. <https://doi.org/10.3354/ame01753>
- Bailey VL, Hicks Pries C, Lajtha K (2019) What do we know about soil carbon destabilization? *Environ Res Lett* 14(8):083004. <https://doi.org/10.1088/1748-9326/ab2c11>
- Barton K (2019). MuMIn: multi-model inference. R package version 1.43.6. <https://CRAN.R-project.org/package=MuMIn>. Accessed 03 Jan 2020
- Bastida F, Eldridge DJ, García C, Kenny Png G, Bardgett RD, Delgado-Baquerizo M (2021) Soil microbial diversity–biomass relationships are driven by soil carbon content across global biomes. *ISME J* 15(7):2081–2091. <https://doi.org/10.1038/s41396-021-00906-0>
- Bolyen E, Rideout JR, Dillon MR, Bokulich NA, Abnet CC, Al-Ghalith GA, Alexander H, Alm EJ, Arumugam M, Asnicar F, Bai Y, Bisanz JE, Bittinger K, Brejnrod A, Brislawn CJ, Brown CT, Callahan BJ, Caraballo-Rodríguez AM, Chase J et al (2019) Reproducible, interactive, scalable and extensible microbiome data science using QIIME 2. *Nat Biotechnol* 37(8):852–857. <https://doi.org/10.1038/s41587-019-0209-9>
- Burnham K, Anderson D (2003) Model selection and multi-model inference. Springer, Cham
- Cavaleri MA, Reed SC, Smith WK, Wood TE (2015) Urgent need for warming experiments in tropical forests. *Glob Change Biol* 21(6):2111–2121. <https://doi.org/10.1111/gcb.12860>
- Chao TT, Zhou L (1983) Extraction techniques for selective dissolution of amorphous iron oxides from soils and sediments. *Soil Sci Soc Am J* 47(2):225–232. <https://doi.org/10.2136/sssaj1983.03615995004700020010x>
- Cismasu AC, Williams KH, Nico PS (2015) Iron and carbon dynamics during aging and reductive transformation of biogenic ferrihydrite (world) [Research-article]. *Am Chem Soc*. <https://doi.org/10.1021/acs.est.5b03021>
- Contosta AR, Burakowski EA, Varner RK, Frey SD (2016) Winter soil respiration in a humid temperate forest: the roles of moisture, temperature, and snowpack. *J Geophys Res Biogeosci* 121(12):3072–3088. <https://doi.org/10.1002/2016jg003450>
- Davidson EA, Janssens IA (2006) Temperature sensitivity of soil carbon decomposition and feedbacks to climate change. *Nature* 440(7081):165–173. <https://doi.org/10.1038/nature04514>
- Delgado-Baquerizo M, Maestre FT, Reich PB, Jeffries TC, Gaitan JJ, Encinar D, Berdugo M, Campbell CD, Singh BK (2016) Microbial diversity drives multifunctionality in terrestrial ecosystems. *Nat Commun*. <https://doi.org/10.1038/ncomms10541>
- Diffenbaugh NS, Scherer M (2011) Observational and model evidence of global emergence of permanent, unprecedented heat in the 20th and 21st centuries. *Clim Change* 107(3):615–624. <https://doi.org/10.1007/s10584-011-0112-y>
- Field C, Raupach M (2004) The global carbon cycle: integrating humans, climate, and the natural world, vol 62. Island Press, Washington
- Gardes M, Bruns T (1993) ITS primers with enhanced specificity for basidiomycetes—application to the identification of mycorrhizae and rusts. *Mol Ecol* 2(2):113–118
- Giardina CP, Litton CM, Asner GP, Crow SE (2014) Warming-related increases in soil CO₂ efflux are explained by increased below-ground carbon flux. *Nat Clim Chang* 4(9):822. <https://doi.org/10.1038/nclimate2322>
- Haaf D, Six J, Doetterl S (2021) Global patterns of geo-ecological controls on the response of soil respiration to warming. *Nat Clim Chang* 11:623–627. <https://doi.org/10.1038/s41558-021-01068-9>
- Hanson PJ, Riggs JS, Nettles WR, Phillips JR, Krassovski MB, Hook LA, Gu L, Richardson AD, Aubrecht DM, Ricciuto DM, Warren JM, Barbier C (2017) Attaining

- whole-ecosystem warming using air and deep-soil heating methods with an elevated CO₂ atmosphere. *Biogeosciences* 14(4):861–883. <https://doi.org/10.5194/bg-14-861-2017>
- Hanson PJ, Griffiths NA, Iversen CM, Norby RJ, Sebestyen SD, Phillips JR, Chanton JP, Kolka RK, Malhotra A, Ole-heiser KC, Warren JM, Shi X, Yang X, Mao J, Ricciuto DM (2020) Rapid net carbon loss from a whole-ecosystem warmed peatland. *AGU Adv.* <https://doi.org/10.1029/2020av000163>
- Hashimoto S, Tanaka N, Suzuki M, Inoue A, Takizawa H, Kosaka I, Tanaka K, Tantasirin C, Tangtham N (2004) Soil respiration and soil CO₂ concentration in a tropical forest, Thailand. *J for Res.* <https://doi.org/10.1007/s10310-003-0046-y>
- Hastie T, Tibshirani R (1986) Generalized additive models. *Stat Sci* 1(3):297–310. <https://doi.org/10.1214/ss/1177013604>
- Heckman K, Hicks Pries CE, Lawrence CR, Rasmussen C, Crow SE, Hoyt AM, von Fromm SF, Shi Z, Stoner S, McGrath C, Beem-Miller J, Berhe AA, Blankinship JC, Keilweit M, Marín-Spiotta E, Monroe JG, Plante AF, Schimel J, Sierra CA, Wagai R (2022) Beyond bulk: Density fractions explain heterogeneity in global soil carbon abundance and persistence. *Global Change Biol* 28:1178–1196. <https://doi.org/10.1111/gcb.16023>
- Henry H (2012) Soil extracellular enzyme dynamics in a changing climate. *Soil Biol Biochem* 47:53–59. <https://doi.org/10.1016/j.soilbio.2011.12.026>
- Hicks Pries CE, Castanha C, Porras RC, Torn MS (2017) The whole-soil carbon flux in response to warming. *Science* 355(6332):1420–1423. <https://doi.org/10.1126/science.aal1319>
- Holmgren G (1967) A rapid citrate-dithionite extractable iron procedure. *Soil Sci Soc A J* 31(2):210–211
- Jackson RB, Lajtha K, Crow SE, Hugelius G, Kramer MG, Piñeiro G (2017) The ecology of soil carbon: pools, vulnerabilities, and biotic and abiotic controls. *Annu Rev Ecol Evol Syst* 48:419–445
- Jobbágy EG, Jackson RB (2000) The vertical distribution of soil organic carbon and its relation to climate and vegetation. *Ecol Appl* 10(2):423–436
- Kimball BA, Alonso-Rodríguez AM, Cavalieri MA, Reed SC, González G, Wood TE (2018) Infrared heater system for warming tropical forest understory plants and soils. *Ecol Evol* 8(4):1932–1944. <https://doi.org/10.1002/ece3.3780>
- Koven CD, Hugelius G, Lawrence DM, Wieder WR (2017) Higher climatological temperature sensitivity of soil carbon in cold than warm climates. *Nat Clim Chang* 7(11):817–822. <https://doi.org/10.1038/nclimate3421>
- Kramer MG, Chadwick OA (2016) Controls on carbon storage and weathering in volcanic soils across a high-elevation climate gradient on Mauna Kea, Hawaii. *Ecology* 97(9):2384–2395. <https://doi.org/10.1002/ecy.1467>
- Lalonde K, Mucci A, Ouellet A, Gélinas Y (2012) Preservation of organic matter in sediments promoted by iron. *Nature* 483(7388):198–200. <https://doi.org/10.1038/nature10855>
- Liu T, Wang B, Xiao H, Wang R, Yang B, Cao Q, Cao Y (2018) Differentially improved soil microenvironment and seedling growth of amorpha fruticosa by plastic, sand and straw mulching in a saline wasteland in Northwest China. *Ecol Eng* 122:126–134. <https://doi.org/10.1016/j.ecoleng.2018.07.030>
- Lu M, Zhou X, Yang Q, Li H, Luo Y, Fang C, Chen J, Yang X, Li B (2013) Responses of ecosystem carbon cycle to experimental warming: a meta-analysis. *Ecology* 94(3):726–738. <https://doi.org/10.1890/12-0279.1>
- Matus F, Rumpel C, Neculman R, Panichini M, Mora M (2014) Soil carbon storage and stabilisation in andic soils: a review. *CATENA* 120:102–110. <https://doi.org/10.1016/j.catena.2014.04.008>
- Mau A, Reed S, Wood T, Cavalieri M (2018) Temperate and tropical forest canopies are already functioning beyond their thermal thresholds for photosynthesis. *Forests* 9(1):47. <https://doi.org/10.3390/f9010047>
- McKeague JA (1967) An evaluation of 0.1 mpyrophosphate and pyrophosphate-dithionite in comparison with oxalate as extractants of the accumulation products in Podzols and some other soils. *Can J Soil Sci* 47:95–99
- Moyes AB, Bowling DR (2013) Interannual variation in seasonal drivers of soil respiration in a semi-arid Rocky Mountain meadow. *Biogeochemistry* 113(1–3):683–697
- Nanzyo M (2002) Unique properties of volcanic ash soils. *Glob Environ Res* 6:99–112
- Nguyen NH, Song Z, Bates ST, Branco S, Tedersoo L, Menke J, Schilling JS, Kennedy PG (2016) FUNGuild: an open annotation tool for parsing fungal community datasets by ecological guild. *Fungal Ecol* 20:241–248
- Nottingham AT, Whitaker J, Turner BL, Salinas N, Zimmermann M, Malhi Y, Meir P (2015) Climate warming and soil carbon in tropical forests: insights from an elevation gradient in the Peruvian Andes. *Bioscience*. <https://doi.org/10.1093/biosci/biv109>
- Nottingham AT, Whitaker J, Ostle NJ, Bardgett RD, McNamara NP, Fierer N, Salinas N, Ccahuana AJQ, Turner BL, Meir P (2019) Microbial responses to warming enhance soil carbon loss following translocation across a tropical forest elevation gradient. *Ecol Lett* 22(11):1889–1899. <https://doi.org/10.1111/ele.13379>
- Nottingham AT, Meir P, Velasquez E, Turner BL (2020) Soil carbon loss by experimental warming in a tropical forest. *Nature* 584(7820):234–237. <https://doi.org/10.1038/s41586-020-2566-4>
- Pachauri RK, Meyer LA, Intergovernmental Panel on Climate Change (eds). (2015) Climate change 2014: synthesis report. Intergovernmental Panel on Climate Change
- Parada AE, Needham DM, Fuhrman JA (2016) Primers for marine microbiome studies. *Environ Microbiol* 18:1403–1414. <https://doi.org/10.1111/1462-2920.13023>
- Peters M, Hemp A, Appelhans T, Becker J, Behler C, Classen A, Detsch F (2019) Climate-land-use interactions shape tropical mountain biodiversity and ecosystem functions. *Nature* 568(7750):88–92
- Plaza C, Pegoraro E, Bracho R, Celis G, Crummer KG, Hutchings JA, Hicks Pries CE, Mauritz M, Natali SM, Salmon VG, Schädel C, Webb EE, Schuur EAG (2019) Direct observation of permafrost degradation and rapid soil carbon loss in tundra. *Nat Geosci* 12(8):627–631. <https://doi.org/10.1038/s41561-019-0387-6>
- Porras RC, Hicks Pries CE, Torn MS, Nico PS (2018) Synthetic Iron (hydr)oxide-glucose associations in subsurface

- soil: effects on decomposability of mineral associated carbon. *Sci Total Environ* 613–614:342–351. <https://doi.org/10.1016/j.scitotenv.2017.08.290>
- Post WM, Kwon KC (2000) Soil carbon sequestration and land-use change: processes and potential. *Glob Change Biol* 6(3):317–327. <https://doi.org/10.1046/j.1365-2486.2000.00308.x>
- R Core Team (2021) R: a language and environment for statistical computing. R Foundation for Statistical Computing, Vienna
- Rasmussen C, Torn MS, Southard RJ (2005) Mineral assemblage and aggregates control carbon dynamics in a California Conifer Forest. *Soil Sci Soc Am J* 69(6):1711–1721. <https://doi.org/10.2136/sssaj2005.0040>
- Rasmussen C, Heckman K, Wieder WR, Keiluweit M, Lawrence CR, Berhe AA, Blankinship JC, Crow SE, Drughan J, Hicks Pries CE, Marin-Spiotta E, Plante AF, Schadel C, Schmid JP, Sierra CA, Thompson A, Wagai R (2018) Beyond clay: towards an improved set of variables for predicting soil organic matter content. *Biogeochemistry* 137(3):297–306. <https://doi.org/10.1007/s10533-018-0424-3>
- Rocci KS, Lavallee JM, Stewart CE, Cotrufo MF (2021) Soil organic carbon response to global environmental change depends on its distribution between mineral-associated and particulate organic matter: A meta-analysis. *Sci Total Environ* 793:148569. <https://doi.org/10.1016/j.scitotenv.2021.148569>
- Ross G, Wang C, Schuppli P (1985) Hydroxylamine and ammonium oxalate solutions as extractants for Fe and Al from soils. *Soil Sci Soc Am J* 49:783–785
- Schädel C, Koven CD, Lawrence DM, Celis G, Garnello AJ, Hutchings J, Mauritz M, Natali SM, Pegoraro E, Rodenhizer H, Salmon VG, Taylor MA, Webb EE, Wieder WR, Schuur EA (2018) Divergent patterns of experimental and model-derived permafrost ecosystem carbon dynamics in response to Arctic warming. *Environ Res Lett* 13(10):105002. <https://doi.org/10.1088/1748-9326/aae0ff>
- Silva JHS, Deenik JL, Yost RS, Bruland GL, Crow SE (2015) Improving clay content measurement in oxidic and volcanic ash soils of Hawaii by increasing dispersant concentration and ultrasonic energy levels. *Geoderma*. <https://doi.org/10.1016/j.geoderma.2014.09.008>
- Silver WL, Lugo AE, Keller M (1999) Soil oxygen availability and biogeochemistry along rainfall and topographic gradients in upland wet tropical forest soils. *Biogeochemistry* 44(3):301–328. <https://doi.org/10.1007/bf00969995>
- Smith DP, Peay KG (2014) Sequence depth, not PCR replication, improves ecological inference from next generation DNA sequencing. *PLoS ONE* 9(2):e90234. <https://doi.org/10.1371/journal.pone.0090234>
- Soong JL, Phillips CL, Ledna C, Koven CD, Torn MS (2020) CMIP5 models predict rapid and deep soil warming over the 21st century. *J Geophys Res.* <https://doi.org/10.1029/2019JG005266>
- Soong JL, Castanha C, Hicks Pries CE, Ofiti N, Porras RC, Riley WJ, Schmidt MWI, Torn MS (2021) Five years of whole-soil warming led to loss of subsoil carbon stocks and increased CO₂ efflux. *Sci Adv.* <https://doi.org/10.1126/sciadv.abd1343>
- Takezawa K (2014) Learning regression analysis by simulation. Springer, Tokyo
- Tang J, Baldocchi DD, Qi Y, Xu L (2003) Assessing soil CO₂ efflux using continuous measurements of CO₂ profiles in soils with small solid-state sensors. *Agric for Meteorol.* [https://doi.org/10.1016/S0168-1923\(03\)00112-6](https://doi.org/10.1016/S0168-1923(03)00112-6)
- Torn MS, Trumbore SE, Chadwick OA, Vitousek PM, Hendricks DM (1997) Mineral control of soil organic carbon storage and turnover. *Nature* 389(6647):170. <https://doi.org/10.1038/38260>
- Torn MS, Chabbi A, Crill P, Hanson PJ, Janssens IA, Luo Y, Hicks Pries C, Rumpel C, Schmidt MWI, Six J, Schrumpf M, Zhu B (2015) A call for international soil experiment networks for studying, predicting, and managing global change impacts. *SOIL* 1(2):575–582. <https://doi.org/10.5194/soil-1-575-2015>
- White T, Bruns T, Lee S, Taylor J, Innis M, Gelfand D, Sninsky J (1990) Amplification and direct sequencing of fungal ribosomal RNA genes for phylogenetics. In: PCR protocols: a guide to methods and applications, Vol 31. Academic Press, New York, pp 315–322. <https://doi.org/10.1016/B978-0-12-372180-8.50042-1>
- Wood S (2006) Generalized additive models: an introduction with R. Chapman and Hall/CRC Press. https://www.researchgate.net/publication/299822741_Generalized_Additive_Models_An_Introduction_With_R. Accessed 03 Jan 2020
- Wood T, Silver WL (2012) Strong spatial variability in trace gas dynamics following experimental drought in a humid tropical forest. *Glob Biogeochem Cycles*. <https://doi.org/10.1029/2010GB004014>
- Wood TE, Cavalieri MA, Reed SC (2012) Tropical forest carbon balance in a warmer world: a critical review spanning microbial- to ecosystem-scale processes. *Biol Rev* 87(4):912–927. <https://doi.org/10.1111/j.1469-185X.2012.00232.x>
- Wood TE, Dettman M, Silver WL (2013) Sensitivity of soil respiration to variability in soil moisture and temperature in a humid tropical forest. *PLoS ONE*. <https://doi.org/10.1371/journal.pone.0080965>
- Wood TE, Cavalieri MA, Giardina CP, Khan S, Mohan JE, Nottingham AT, Reed SC, Slot M (2019) Soil warming effects on tropical forests with highly weathered soils. *Ecosyst Conseq Soil Warm.* <https://doi.org/10.1016/b978-0-12-813493-1.00015-6>
- Xu W, Yuan W, Dong W, Xia J, Liu D, Chen Y (2013) A meta-analysis of the response of soil moisture to experimental warming. *Environ Res Lett* 8(4):044027. <https://doi.org/10.1088/1748-9326/8/4/044027>
- Zimmermann M, Meir P, Bird MI, Malhi Y, Ccahuana AJQ (2010) Temporal variation and climate dependence of soil respiration and its components along a 3000 m altitudinal tropical forest gradient. *Glob Biogeochem Cycles*. <https://doi.org/10.1029/2010GB003787>

Publisher's Note Springer Nature remains neutral with regard to jurisdictional claims in published maps and institutional affiliations.